Double-grating polarizer for terahertz radiation with high extinction ratio

Lin Sun,* Zhi-Hui Lv, Wei Wu, Wei-Tao Liu, and Jian-Min Yuan

Department of Physics, National University of Defense Technology, Changsha 410073, China

*Corresponding author: sunlin@nudt.edu.cn

Received 8 December 2009; revised 12 February 2010; accepted 15 March 2010;
posted 15 March 2010 (Doc. ID 121125); published 2 April 2010

We propose a layout of a high extinction ratio polarizer in the terahertz (THz) domain. This polarizer is composed of two dense metal wire gratings separated in parallel, of which the grating constant is much smaller than the incident wavelength. Numerical analysis shows that, in the range of 0.3 THz – 3 THz, the transmission of TM wave through this polarizer is higher than 97% and the extinction ratio achieved is about 180 dB—much higher than the conventional wire-grid polarizer. © 2010 Optical Society of America

OCIS codes: 050.0050, 050.2230.

1. Introduction

As terahertz (THz) generation and detection techniques develop, demand for the ability to control and manipulate THz waves is increasing [1,2]. Many materials inherently do not respond to THz radiation, so artificially structured subwavelength devices called "plasmonic devices," which have potential applications for THz emitters, detectors, waveguides, splitters, mirrors, and lenses, gained a lot of attention [3]. One application is manipulation of the polarization state of THz radiation. Though the conventional wire-grid polarizer is widely used and commercially available [4], the extinction ratio is not high enough for some applications. To improve the extinction ratio, a plate polarizer composed of a stack of silicon and air layers was suggested [5], reaching the maximum extinction ratio of 50 dB. However, it is only in the frequency range of 0.1 – 0.15 THz. By inserting a nematic liquid crystal layer into fused silica, a Feussner-type THz polarizer was designed, working in the frequency range of 0.2 – 1 THz with a high extinction ratio. Nevertheless, the assembled polarizer could not be made compact [6]. More recently, using the rigorous coupled-wave analysis theory combined with the Brewster angle effect, a micrometer-pitch wire-grid polarizer was designed and fabricated, of which the measured extinction ratio was over 23 dB in 0.5 – 3 THz [7]. In order to break the limitation of the finer wire width of the conventional wire-grid polarizer in THz, a dual-layer frequency-selective grid polarizer for ease of fabrication was presented [8]. Actually, transmission characteristics of double-grating and its application as Fabry–Perot (FP) interferometers had been deeply discussed in the 1970s [9]. The theory and practical application of FP interferometers used at submillimeter wavelengths were reviewed in 1982 [10], where metallic meshes and grids were used as high reflectors for FP. Until the beginning of the twenty-first century, dual-layer grids used for polarizer of high performance in optical and infrared regions were verified and fabricated [11–14], attributed to the development of nanolithographic technology. However, for the convenience of nanoscale fabrication, misaligned bilayer metal wire gratings were widely used, where the fill factors of upper and lower layers of metal grids complement each other (they always add up to 1). Hence, the fill factor is usually set at 0.5 in the transmission polarizer, which actually limits the enhancement of the extinction ratio [12–14].

In order to get a broadband polarizer of high extinction ratio in the THz region, we investigate

0003-6935/10/112066-06$15.00/0

and optimize the performance of a double-grating polarizer (DGP). Through effective media theory (EMT) calculation, we found that not only the amplitude but also the phase of reflectance from wire grating are quite different between two orthogonal polarization waves [the polarization direction of the TE wave is parallel to grating wires, and the TM wave is perpendicular, as shown in Fig. 1]. A conventional wire-grid polarizer uses the amplitude difference to get high TM transmission and low TE transmission. In the case of FP interference, the amplitude of reflectance decides the finesse, and phase decides the transmission intensity. Making use of this point, we realize the TM constructive interference and TE destructive interference at the same time in a wide frequency range. Adjusting the geometric parameters with finite element method (FEM) simulation, we optimize the DGP to achieve a more than 97% TM transmission and an over 180 dB extinction ratio in the frequency range of 0.3 – 3 THz. In the final part of this paper, considering the practical fabrication and application, we do some simulation about the lateral shift and relative inclination between two layers of gratings. Results show that lateral shift hardly influences the performance, and in a range of 200 μm, an inclination of 5° is tolerable.

2. Theory Model and Simulation Method

A geometrical description of the DGP construction is shown in Fig. 1. The cross section of each wire is assumed to be rectangular. Since the wavelength of the incident wave is much greater than the dimensions of the construction, it is possible to regard the wire grating as being a homogeneous lamella [15]. Theoretical derivations of this effective medium process could be found in Ref. [16]. For the normal incidence, the effective refractive indices n_{TM} and n_{TE} for the TM and TE wave are as follows [15]:

$$n_{\mathrm{TM}} = [f/\varepsilon_{\mathrm{m}} + (1-f)/\varepsilon_0]^{-1/2}$$
$$n_{\mathrm{TE}} = [f\varepsilon_{\mathrm{m}} + (1-f)\varepsilon_0]^{1/2}, \quad (1)$$

here, the fill factor $f = w/P$ is defined as the ratio of the width of metal wire w to the grating constant P. ε_{m} and ε_0 are the relative permittivity of metal and air, respectively. In the case of a dense metallic wire grating, only the zeroth order propagation is considered. According to the Fresnel formula and the interference effect inside the wire grating [17], the zeroth-order reflection and transformation coefficients for TM and TE wave could be obtained. Then the total transmission coefficient through the FP instrument is as follows [9]:

$$\tau = \frac{t^2}{1 - r^2\exp(j\varphi)}, \quad (2)$$

where t and r, respectively, represent the zeroth order transformation and reflection coefficient of the equivalent lamella. For normal incidence, $\varphi = \frac{4\pi n_0 S}{\lambda}$, where S is the spacing between two layers of gratings in the DGP. n_0 is the effective refractive index of the interference media. The total transmitted intensity is [9]

$$|\tau|^2 = \frac{1}{1 + F\sin^2\xi}, \quad (3)$$

where $\xi = \varphi/2 + \arg(r)$, and the term F, well known as the finesse of the interferometer, is defined as

$$F = \frac{4|r|^2}{(1-|r|^2)^2}, \quad (4)$$

for normal incidence, constructive interference occurs when

$$\xi = m\pi, \quad (5)$$

here, m is an integer specifying the order of interference.

For a homochromatic wave, $\arg(r)$ of the two orthogonal polarization waves (TM and TE) are quite different from each other. When $f = 0.8$, $h = 0.5\,\mu$m, $\lambda = 300\,\mu$m, and $\varepsilon_{\mathrm{m}} = -1.12\times10^5 + i\times7.22\times10^5$ (relative permittivity of Ag at 1 THz [18]), the difference of $\arg(r)$ between TM and TE achieved 88.3°, nearly half the period of function (3). Changing the frequency of the incident wave, we found that the result changes a little, from 89.5° at 0.3 THz to 85° at 3 THz. This means that in the large frequency range for DGP, when the TM wave interferes constructively, the TE wave interferes destructively, and vice versa. This could be confirmed in Fig. 2, in which a cyclic behavior of transmittance with a period of 100 μm at a fixed wavelength of 200 μm can be observed with the increasing spacing S. However, for a given DGP, because the phase ξ changes with wavelength, not all the frequency components would simultaneously interfere constructively or destructively. Fortunately, for dense metallic wire grating, owing to the high reflectance of TE and the high transmittance of TM, the TE interference fringe is sharp and narrow, while TM is smooth and wide, just as demonstrated in Fig. 2, which reveals that for a wideband of spacing S in one period, TE transmission is strongly suppressed while TM transmission is enhanced. That is the reason why we use DGP to enhance the extinction ratio in a wide frequency range.

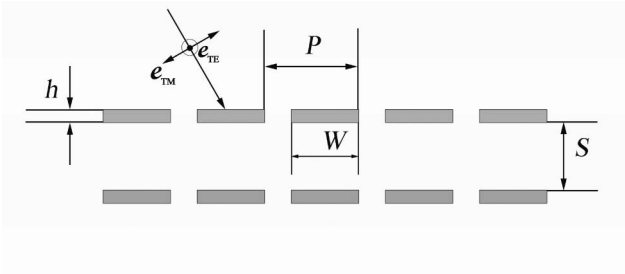

Fig. 1. DGP: rectangles filled with gray color, metal wires; P, wire period; S, spacing between two layers of gratings; h, wire depth; and w, metal wire width.

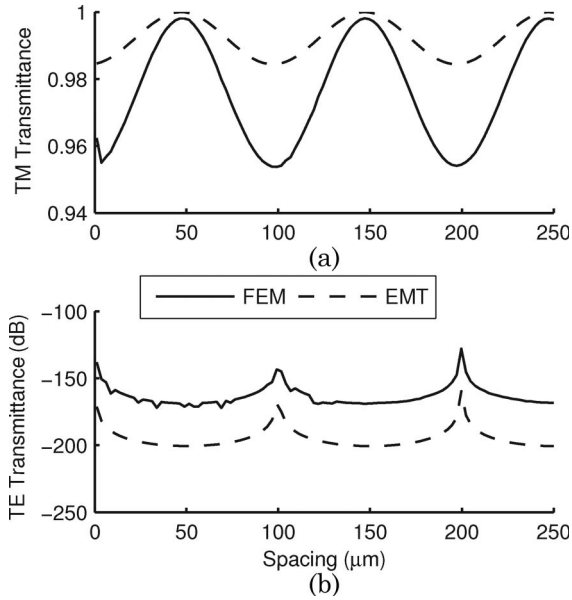

Fig. 2. (a) TM and (b) TE transmittance for DGP as a function of spacing. The wavelength is 200 μm, the fill factor is 0.8, and the wire depth is 1 μm. Solid curve, FEM result; dotted curve, EMT result.

Additionally shown in Fig. 2 is the result of FEM simulation, which is coincident with the result of EMT. Nevertheless, the two results do not agree with each other completely. Because the zeroth-order approximation of EMT relies on a spatial average but ignores the fine geometry of inhomogeneity [16], the application of EMT is inadequate to investigate the effects of geometric parameters on the performance of DGP, even when the wavelength is much larger than the geometric dimensions. Therefore, in the following analysis, we will apply the FEM instead.

In FEM simulation, we use gold as the wire material and air as the background material. Since, in the THz region, free electrons in the metal are considered as classical charges subject to random collisions, we use the simple Drude model for conductivity of metal material [7]:

$$\sigma = \frac{N{q_e}^2}{m(\gamma - i\omega)}, \tag{6}$$

here, N is the number of free electrons per unit volume, q_e is the charge of an electron, m is the mass of the electron, γ is the damping constant, and ω is the angle frequency.

For simplicity, we simulate the model in 2D space. The calculation domain is set in 10 grating periods, with Floquet periodic boundaries to simulate infinitely arranged gratings. Plane waves of different frequencies are illuminated in from one port, through the structure, and out another port. The magnetic field is calculated for the TM wave and the electric field for the TE wave.

3. Results and Discussions

Under the normal incidence, over the frequency range from 0.3 to 3.0 THz, the transmission spectra of the TM wave for various periods of metal wire grating are shown in Fig. 3(a) for a DGP and Fig. 3(b) for a single-grating polarizer (SGP). Geometric parameters are set: fill factor $f = 0.9$, spacing $S = 25\,\mu$m, and wire depth $h = 1\,\mu$m. The spectra show a number of distinct features. Several resonant peaks are observed for DGP, which shift blue and become stronger when the grating constant P decreases. The blueshift is mainly because of the change of the reflectance phase $\arg(r)$ in Eq. (2), which is responsible for resonant frequency. The wider and stronger shape comes from the higher transmittance of the corresponding SGP, shown in Fig. 3(b), which supplies background transmission for DGP interference. Another remarkable feature is that the number of the peak in the spectrum increases while the grating constant P increases. It is actually the result of reduced distance between two neighboring peaks in the spectrum. According to FP interference theory, each peak is indicated by a different order of interference, leading to a phase difference of π one by one. For

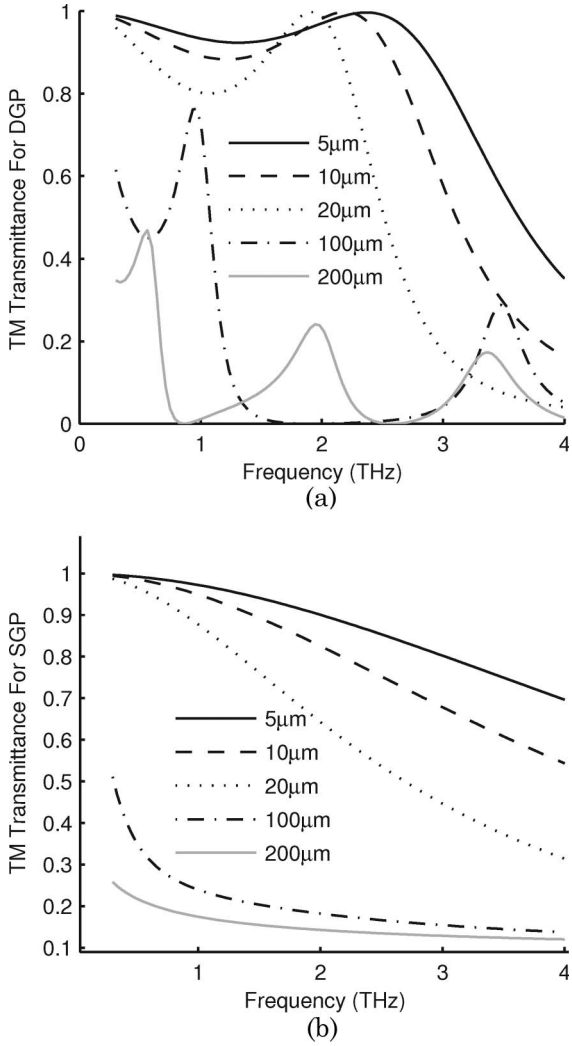

Fig. 3. TM transmittance spectra for 5 μm, 10 μm, 20 μm, 100 μm, and 200 μm periods. (a) Spectra of DGP. (b) Spectra of corresponding SGP.

a fixed spacing S, the reduced distance between neighboring peaks necessarily corresponds to the enhanced effective refraction index of media. This might be induced by resonant interaction between the wave and the metal structure, which could even cause negative index as the parameters are chosen properly [19,20]. As for TE wave, the first-order interference occurs at about 6 THz on the condition of 25 μm spacing. In the frequency under consideration, the TE wave is strongly suppressed and transmission decreases with the period P, where it is −50 dB for period of 200 μm and −190 dB for 5 μm. So from the discussion above, it is obvious that the smaller the period of grating, the better the property of DGP.

The fill factor is also a key parameter that determines the performance of DGP. As shown in Fig. 4(b), the extinction ratio [defined as $10\log(T_{\mathrm{TM}}/T_{\mathrm{TE}})$] gets higher generally with a bigger fill factor [7]. However, as illuminated in Fig. 4(a), when the fill factor increases, the TM transmittance decreases sharply away the constructive interference, reducing the whole transmission efficiency. Consequently, there is a trade-off between the TM transmittance and extinction ratio that we must consider. Coarsely evaluated, it will be good to set the fill factor in the range of 0.8 – 0.9.

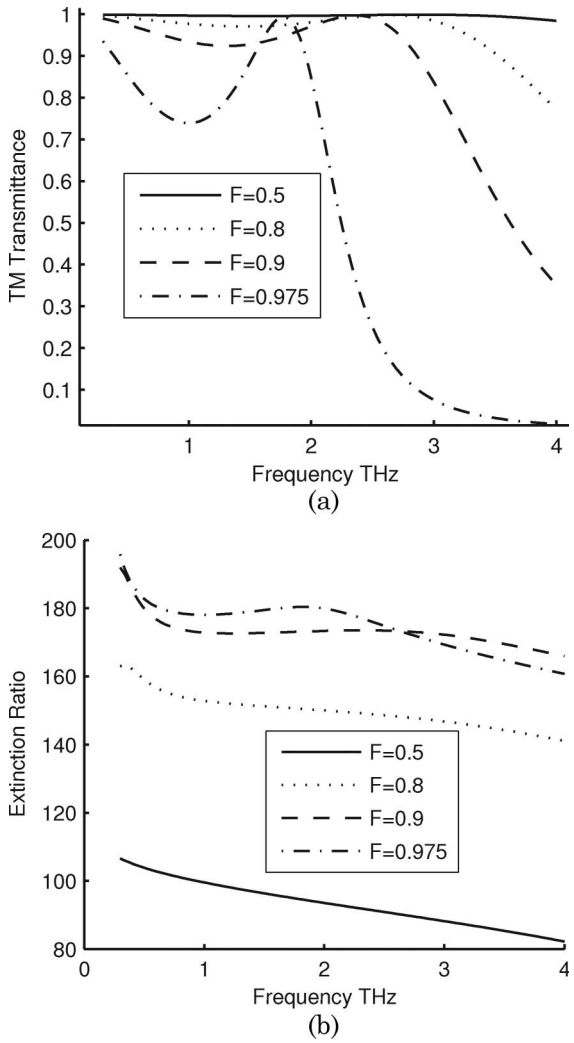

Fig. 4. (a) TM transmittance and (b) extinction ratio for DGP with various fill factors. The spacing is 25 μm, the period is 5 μm, and the wire depth is 1 μm.

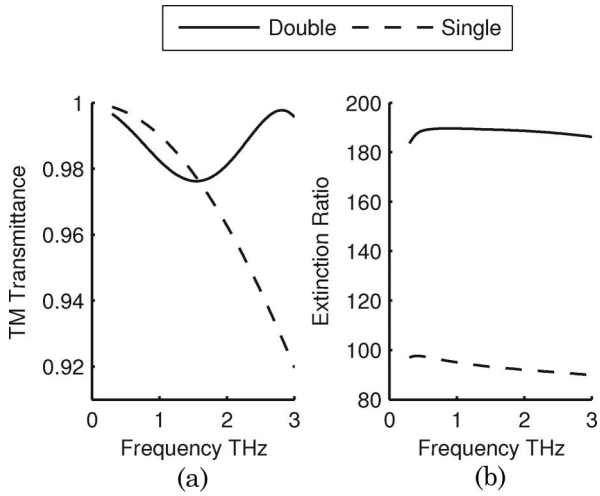

Fig. 5. (a) TM transmittance and (b) extinction ratio for DGP (solid curve) and SGP (dotted curve) with optimized geometric parameters (period of 3 μm, fill factor of 0.8, wire depth of 1 μm, and spacing of 24 μm).

In order to get the best performance of the DGP, the geometric parameters of the construction are optimized by FEM. Figure 5 shows the optimized TM transmittance and extinction ratio as a function of frequency. For direct comparison, the property of the corresponding SGP is shown also. Optimized geometric parameters are set as grating constant $P = 3\,\mu$m, fill factor $f = 0.8$, wire depth $h = 1\,\mu$m, and spacing between the two layers of grating $S = 24\,\mu$m. The simulation results show that DGP almost enhances the extinction ratio as much as twice of that for SGP.

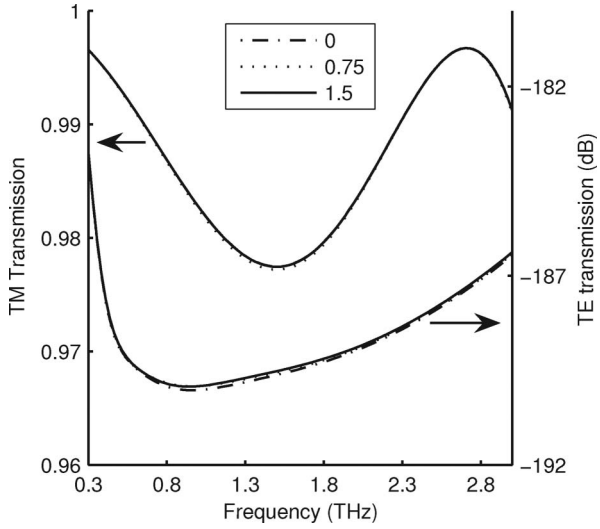

Fig. 6. TM and TE transmittance through optimized DGP with various lateral shifts. Dashed-dotted curve is of zero lateral shift, dotted curve is of 0.75 μm lateral shift (a quarter of the period), and solid curve is of 1.5 μm lateral shift (half of the period).

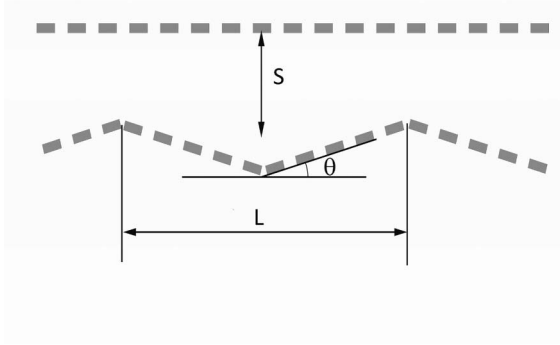

Fig. 7. Geometric depiction for corrugated DGP: θ, inclination angle; L, corrugation period; S, spacing of original parallel gratings.

Additionally, the TM transmittance for DGP does not decrease with increasing frequency monotonously as for SGP, but reaching the minimum value of 97.6% at 1.5 THz and achieving 99.8% around 3 THz. This feature improves the property of a conventional wire-grid polarizer in the higher frequency region.

In practical fabrication of the DGP, there might be some afflicting influence that should be taken account into. In the following section, lateral shift and relative inclination between two layers of gratings are introduced.

In the frequency considered, noting that the surface plasmon polariton, which is the main reason of peak transmission dependence on lateral shift in double-layer metallic slit arrays [21,22], is not excited in the SGP here in our design [see Fig. 3], it could be expected that a lateral shift of the DGP with equivalent dimensions consequently has little impact on the performance. Two groups of simulation results in Fig. 6 confirmed this point of view. TM transmissions with a different lateral shift (0, 1/4, and 1/2 of grating period) superposition each other, and so do the corresponding extinction ratios.

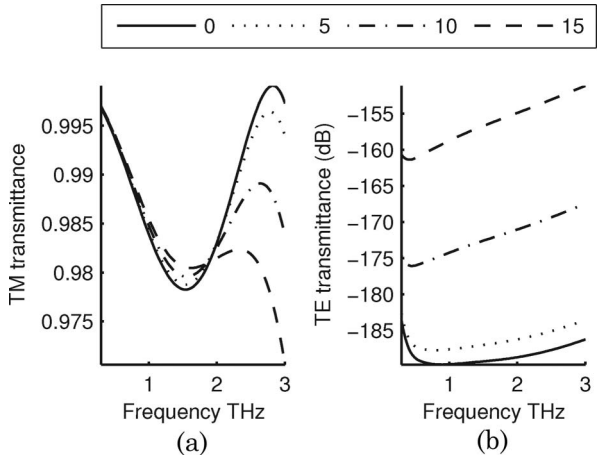

Fig. 8. (a) TM and (b) TE transmittance spectra for corrugated DGP with inclination angles of 0°, 5°, 10°, and 15°. The grating period is 3 μm, the fill factor is 0.8, parallel spacing is 24 μm, and wire depth is 1 μm.

As for the case of relative inclination, a special layout is brought out to investigate the influence. The geometric form is depicted in Fig. 7. One layer of metal wires is aligned along a corrugated surface instead of the original plane surface. The corrugation period L is set at 200 μm, while the inclination angle θ is varied. From the results shown in Fig. 8, it could be seen that the performance of the polarizer reduces rapidly with the inclination angle, where TM transmission decreases by 0.3% with 5° and 3% with 15°, and TE transmission increases by 3 dB with 5° and 30 dB with 15°. Analyzing the original and reduced performance, we see that the inclination angle of about 5° is tolerable.

On the basis of the above discussions, it could be concluded that the requirement for perfect alignment of two layers of gratings needs not be fulfilled critically. This makes the fabrication of DGP feasible and flexible.

4. Conclusion

In conclusion, a very simple approach for a high extinction ratio polarizer in THz frequency domain is discussed. It mainly utilizes the FP interference effect and polarization sensitive response of metal wire gratings. Since the dimensions of the construction are extremely smaller than the wavelength considered, the EMT is used to exploit the underlying physical reason. Using the FEM, the DGP is optimized, with a fill factor of 0.8, a wire depth of 1 μm, a period of 3 μm, and a spacing of 24 μm. The TM transmittance is over 97.6%, and the extinction ratio reaches 180 dB in the frequency range from 0.3 to 3 THz. It is found that the DGP behaves well, even when the alignment and flatness are not completely fulfilled, which makes the fabrication of DGP feasible and flexible.

This work is supported by the National Natural Science Foundation of China (NSFC) under grants 10734140 and 60621003, and the National Basic Research Program of China (973 Program) under grant 2007CB815105.

References

1. M. Tonouchi, "Cutting-edge terahertz technology," Nat. Photon. **1**, 97–105 (2007).
2. T. Loffler, K. J. Siebert, N. Hasegawa, T. Hahn, and H. G. Roskos, "All-optoelectronic terahertz imaging systems and examples of their application," Proc. IEEE **95**, 1576–1582 (2007).
3. M. Dragoman and D. Dragoman, "Plasmonics: applications to nanoscale terahertz and optical devices," Prog. Quantum Electron. **32**, 1–41 (2008).
4. A. E. Costley, K. H. Hursey, G. F. Neill, and J. M. Ward, "Free-standing fine-wire grids: their manufacture, performance, and use at millimeter and submillimeter wavelengths," J. Opt. Soc. Am. **67**, 979–981 (1977).
5. S. Awasthi, A. Srivastava, U. Mlaviya, and S. P. Ojha, "Wide-angle, broadband plate polarizer in terahertz frequency region," Solid State Commun. **146**, 506–509 (2008).
6. C.-F. Hsieh, Y.-C. Lai, P.-P. Panand, and C.-L. Pan, "Polarizing terahertz waves with nematic liquid crystals," Opt. Lett. **33**, 1174–1176 (2008).

7. I. Yamada, K. Takano, M. Hangyo, M. Saito, and W. Watanabe, "Terahertz wire-grid polarizers with micrometer-pitch Al gratings," Opt. Lett. **34**, 274–276 (2009).
8. V. Yurchenko, J. Murphy, J. Barton, J. Verheggen, and K. Rodgers, "Dual-layer frequency-selective grid polarizers on thin-film substrates for THz applications," in *Proceedings of the 38th European Microwave Conference, 2008, EuMC 2008* (IEEE, 2008), pp. 1014–1017.
9. J. L. Adams and L. C. Botten, "Double gratings and their applications as Fabry–Perot interferometers," J. Opt. **10**, 109–117 (1979).
10. E. A. M. Baker and B. Walker, "Fabry–Perot interferometers for use at submillimetre wavelengths," J. Phys. E: Sci. Instrum. **15**, 25–32 (1982).
11. Z. Yu, P. Deshpande, W. Wu, J. Wang, and S. Y. Chou, "Reflective polarizer based on a stacked double-layer subwavelength metal grating structure fabricated using nanoimprint lithography," Appl. Phys. Lett. **77**, 927–929 (2000).
12. Y. Ekinci, H. H. Solak, C. David, and H. Sigg, "Bilayer Al wire-grids as broadband and high-performance polarizers," Opt. Express **14**, 2323–2334 (2006).
13. S. H. Ahn, J.-S. Kim, and L. J. Guo, "Bilayer metal wire-grid polarizer fabricated by roll-to-roll nanoimprint lithography on flexible plastic substrate," J. Vac. Sci. Technol. B **25**, 2388–2391 (2007).
14. Z. Y. Yang, M. Zhao, N. L. Dai, G. Yang, H. Long, Y. H. Li, and P. X. Lu, "Broadband polarizers using dual-layer metallic nanowire grids," IEEE Photon. Technol. Lett. **20**, 697–699 (2008).
15. F. Flory, L. Escoubas, and B. Lazarides, "Artificial anisotropy and polarizing filters," Appl. Opt. **41**, 3332–3335 (2002).
16. P. Lalanne and D. Lemercier-Lalanne, "On the effective medium theory of subwavelength periodic structures," J. Mod. Opt. **43**, 2063–2085 (1996).
17. F. Träger, *Handbook of Lasers and Optics* (Springer, 2007).
18. H. Xiao-Yong and C. Jun-Cheng, "Investigation on transmission properties of terahertz wave through semiconductor aperture," Commun. Theor. Phys. **49**, 485–488 (2008).
19. V. M. Shalaev, W. Cai, U. K. Chettiar, H.-K. Yuan, A. K. Sarychev, V. P. Drachev, and A. V. Kildishev, "Negative index of refraction in optical metamaterials," Opt. Lett. **30**, 3356–3358 (2005).
20. C. Imhof and R. Zengerle, "Strong birefringence in left-handed metallic metamaterials," Opt. Commun. **280**, 213–217 (2007).
21. H. B. Chan, Z. Marcet, Kwangje Woo, and D. B. Tanner, "Optical transmission through double-layer metallic subwavelength slit arrays," Opt. Lett. **31**, 516–518 (2006).
22. R. Ortuño, C. García-Meca, F. J. Rodríguez-Fortuño, J. Martí, and Alejandro Martínez, "Role of surface plasmon polaritons on optical transmission through double layer metallic hole arrays," Phys. Rev. Lett. **79**, 075425 (2009).